STATISTICAL ANALYSIS OF OCEAN WAVE AND WIND PARAMETERS RETRIEVED WITH AN EMPIRICAL SAR ALGORITHUM

G. Song[(1),(2)], S. Lehner[(2)], J. Schulz-Stellenfleth[(2)] , H. Grassl[(1)]
[(1)]University of Hamburg, Bundesstrasse 53, 20146 Hamburg, Email:guiting.song@dlr.de
[(2)]DLR, Oberpfaffenhofen, 82230 Wessling

ABSTRACT

A global dataset of two years (September 1998 to December 2000) of ERS SAR data was reprocessed to more than one million SAR imagettes. Met ocean Parameters like significant ocean wave height (H_s), wind speed (U_{10}) and mean wave period (T_{m-10}) are derived from the SAR images using a new empirical algorithm CWAVE [1]. The results are compared to collocated ERS altimeter data and in Situ measurements from NOAA buoys and observations taken onboard the vessel Polarstern.
It is shown that the SAR derived H_s is comparable in quality to altimeter measurements and can thus be used for real time assimilation.

1. INTRODUCTION

In state of the art ocean wave models like the WAM model (WAMDI report) the full two-dimensional ocean wave spectrum is predicted. Derived parameters are, e.g., significant wave height and mean and peak wavelength of the spectrum.
SAR images can be used to derive the full two dimensional ocean wave spectrum by nonlinear inversion techniques using standard SAR algorithms, e.g. the MPI algorithm used at ECMWF, the standard ESA algorithm and the PARSA algorithm [2], [3], [4]. All of the algorithms need model information as a first guess.
The Synthetic Aperture Radar (SAR) onboard the European Satellite ERS-2 is operated in wave-mode over the global oceans, whenever no image-mode acquisition (100km × 100km) is requested. Conventionally image spectral information from these (5km × 10km) wave mode data is delivered as an ESA product, the two dimensional UWA image spectra, which are used at weather centres to measure ocean waves over the global oceans in real time. The SAR image spectra are used together with first guess information from a wave model to derive two dimensional ocean wave spectra in order to improve ocean wave forecast [1].
The original 5 km × 10km ERS SAR images that contain information on a variety of additional geophysical parameters like sea ice parameters, sea surface features, wind speed and direction, and individual ocean wave parameters are only for the follow up Satellite ENVISAT stored at ESA for further investigation [5]. For the studies performed in this paper, the ERS SAR raw data had thus to be reprocessed to SAR images. Then the empirical algorithm CWAVE is used on the SAR images to derive integral spectral parameters and wind speed.
The results derived are then compared to in Situ data and altimeter satellite data that are already assimilated, e.g., at ECMWF to improve the model predictions. For the wind field these are observations of the wind field from scatterometer data [6], [7] and significant wave height from the altimeter [8]. The altimeter H_s data used in this study are provided by OCEANOR wave climate products.
The main goal of this paper is to validate CWAVE and to compare the CWAVE derived parameters to altimeter and ECMWF model rusults.

2. STATISTICAL COMPARISON TO ERA 40 MODEL RESULTS

ERA-40 datasets could be found at website: http://data.ecmwf.int/data/d/era40_daily/. ERA 40 data contain daily and monthly analysis and forecast values interpolated to a 2.5° × 2.5° regular grid. The collocation distance to the SAR imagettes is thus less than 1.25°. In this study H_s is extracted from ERA-40 GRIB type datasets at the four synoptic times 00:00, 06:00, 12:00 and 18:00 UTC each day. The temporal gap between ERA 40 and SAR results is thus less than 3 hours.

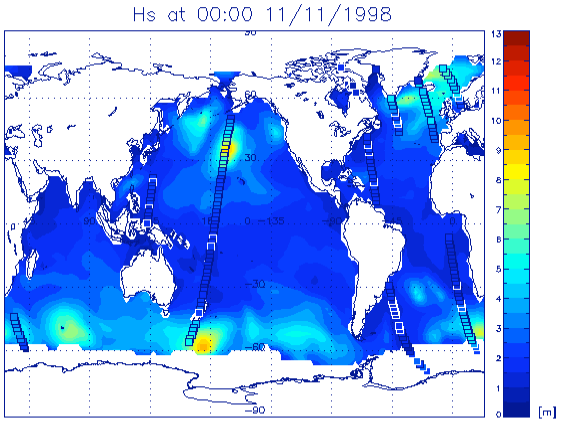

Figure 1 Results of the SAR CWAVE algorithm for significant wave height in comparison to ERA 40 model results

Proc. 'Envisat Symposium 2007', Montreux, Switzerland
23–27 April 2007 (ESA SP-636, July 2007)

The SAR results are compared to the collocated ERA-40 data. Fig. 1 shows examples of the comparison with the SAR results superimposed on the map of the ERA-40 results. The colored square is the significant wave height H_s derived from SAR data, the background map shows H_s from the ECMWF ERA 40 model. SAR images are tested for homogeneity and images that show surface features disturbing the image spectrum are sorted out in later comparisons. Squares with a white frame mark inhomogeneous imagettes, squares with black frame are homogeneous and used for wind and sea state measurements. For further information on the inhomogeneity test see [9].

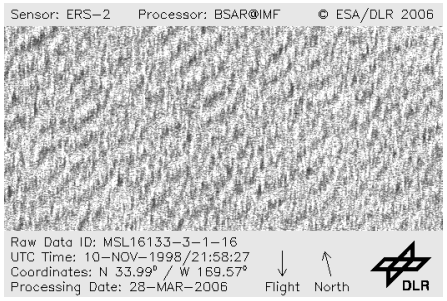

Figure 2 Example of an imagette acquired on November 10, 1998, at 21:58, corresponding to the nearest synoptic time as given in figure 1.

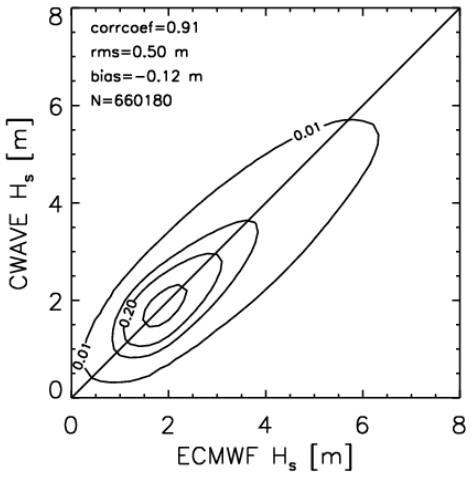

Figure 3 Scatterplot of ERA 40 significant wave height H_s against SAR CWAVE and CWIND results for all homogeneous wave mode SAR images

Two years of SAR images from September, 1998 to December, 2000 were collocated with ERA 40 model results. As an example in fig. 1 both SAR and ERA-40 data show the storm situated over the North Pacific with significant wave height up to 9 meters as measured by CWAVE 1.0. Fig. 2 shows the corresponding imagette of the storm in the north Pacific. In fig. 3 the statistical relationship of H_s between the SAR and ERA-40 data is shown. Significant wave height shows an rms of 0.6 meters with a high correlation of 0.9. Further updates of the empirical algorithm CWAVE based on new tuning data sets will be investigated.

3. VALIDATION OF CWAVE AND CWIND

3.1 COMPARISON WITH BUOY MEASUREMENTS

SAR measurements are validated by buoy data, which are available from National Oceanic and Atmospheric Administration's (NOAA) National Data Buoy Centre (NDBC) providing hourly observations. When taking the collocation distance between SAR imagettes and buoy to be less than 100 km and the temporal gap between them within 1 hour, then the 96 collocations are available.

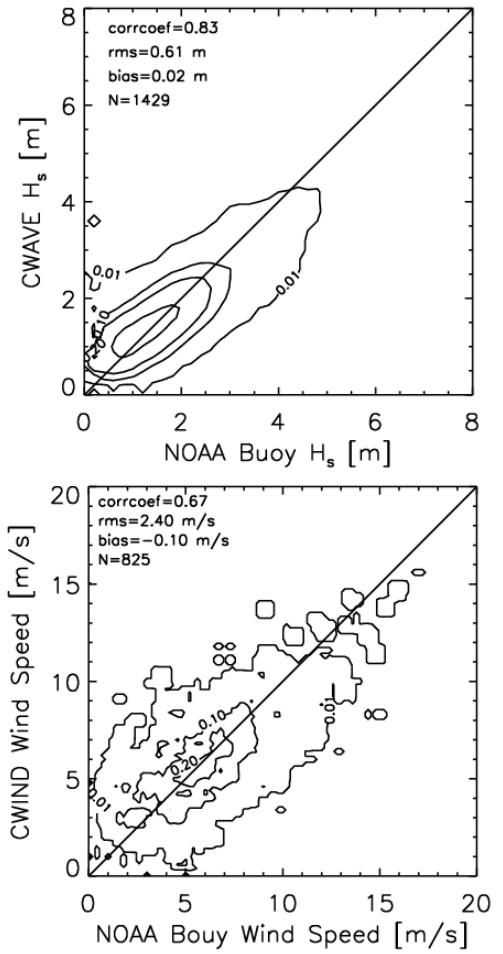

Figure 4 Validation of the CWAVE algorithm against NOAA buoys for H_s and U_{10}

Fig. 4 shows the statistical analysis result between the SAR results and buoy measurements for H_s and U_{10}. Using all available buoy collocations in the regression the root mean square (rms) is 0.61 m for significant wave height. By taking only deep water buoys into account (water depth which larger than 100 m) the error goes down to 0.5m. Further improvement by taking additionally the CMOD into account could be achieved.

3.2 COMPARISON TO OBSERVATIONS ON THE VESSEL POLARSTERN

Since the end of 1982 a meteorological observatory programme has been carried out on board the research vessel Polarstern. The wind vector is measured by instrument on board Polarstern and H_s is estimated by personal observation on the Polarstern. Figure 5 shows the H_s and U_{10} comparison between CWAVE SAR, ERA-40 and Polarstern data for March, 27, 2000.

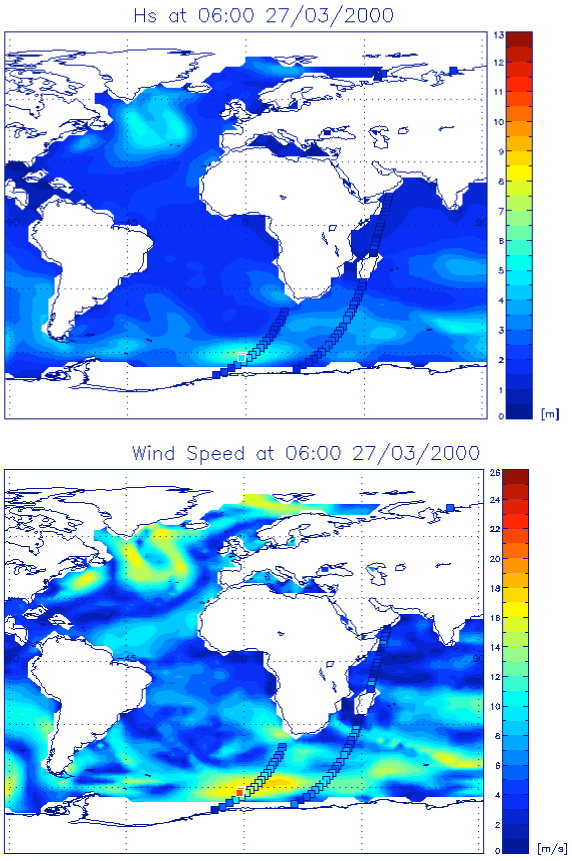

Figure 5 Example of a comparison between observations done on board the vessel Polarstern (AWI) together with SAR measurements and ERA 40 model results

The square framed black is the H_s and U_{10} derived from SAR, the square framed white is the H_s and U_{10} as observed by vessel Polarstern and the background contour is the ERA 40 results. All of these three different data show a storm situate in the South Atlantic, one of the strongest the Polarstern met during the two respective years of travelling. Fig. 6 shows H_s observed on vessel Polarstern from September 1998 to December 2000; Fig. 7 shows U_{10} measured by Polarstern the same time period as H_s. From these two figures we could know that Vessel Polarstern observed few storm mainly on account of safety.

Fig. 8 shows one SAR imaggete nearest to the Polarstein vessel measurement. Fig. 9 shows the statistical analysis between SAR and Polarstern data. The collocation distance between SAR imagettes and Polarstern data is less than 300 km and the temporal gap between them is within 1 hour.

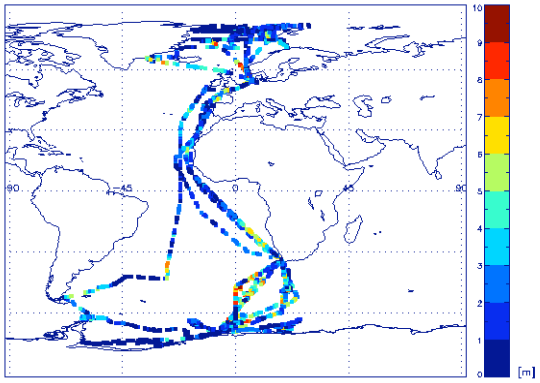

Figure 6 H_s observed on vessel Polarstern from September 1998 to December 2000

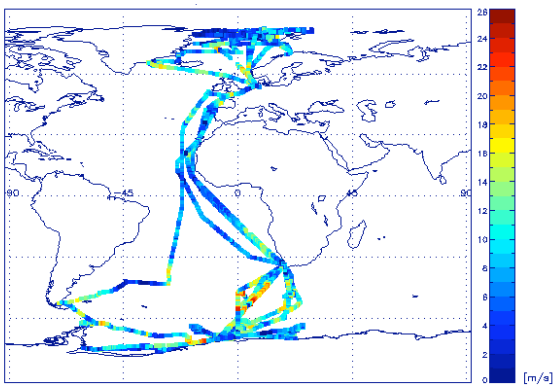

Figure 7. U_{10} measured by vessel Polarstern from September 1998 to December 2000

Fig. 10 shows the H_s statistical analysis between SAR, ECMWF, altimeter and Polarstern vessel data. The distribution of SAR, ECMWF and Altimeter results are

similar, however the peak of Polarstern data is lower than the other three data mainly because the Polarstern vessel avoids danger in case of storm and seldom passes through the storm region.

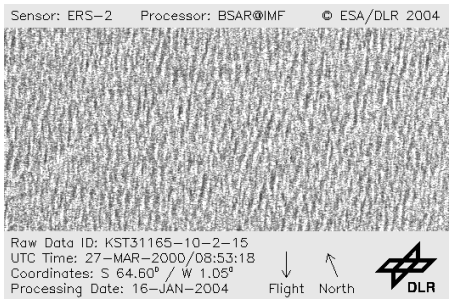

Figure 8 The imagette closest to the Polarstern observations from figure 5.

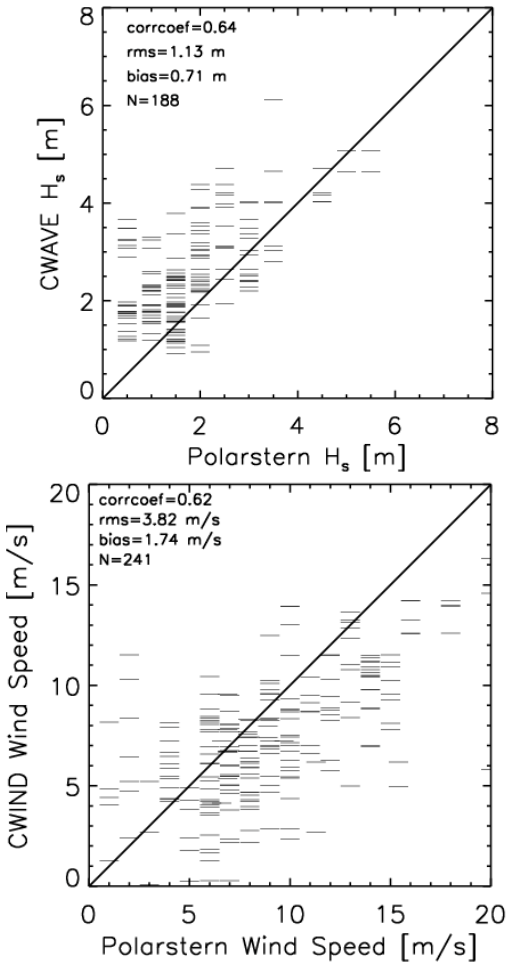

Figure 8 Validation of the CWAVE algorithm against Polarstern observations

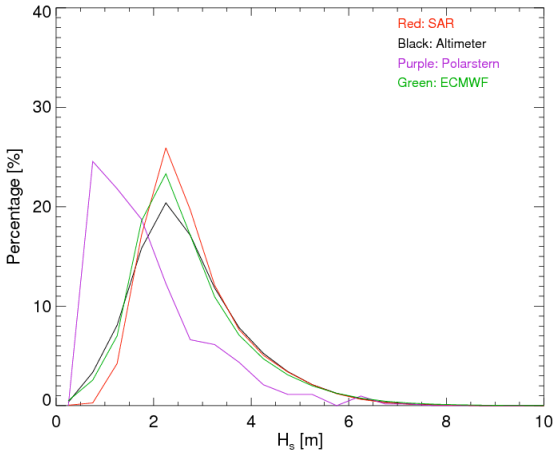

Figure 10 Histogram of measurements of significant wave height by CWAVE SAR, altimeter, Polarstern and ERA 40.

4. COMPARISON BETWEEN SAR RESULT AND OTHER DATA

4.1 COMPARISON OF CWAVE SAR TO ERS ALTIMETER MEASUREMENTS

Fig. 11 shows the scatterplot of H_s between the SAR and altimeter results for the whole year of 1999. It can be seen that H_s derived from altimeter is slightly higher than that measured by CWAVE SAR, especially for high values of H_s. It is concluded that the tuning data set for CWAVE may not have contained enough high wind speed cases. As an example fig. 12 shows a map for the comparison of SAR, ERA-40 and altimeter data for February, 25, 1999.

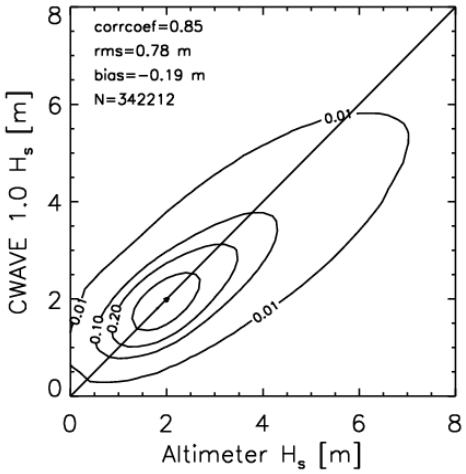

Figure 11 Scatterplot of altimeter derived significant wave height against CWAVE SAR results

Fig. 13 shows the comparison of the data for one orbit across the North Atlantic from fig. 12. For wave heights below 5 meters agreements is very good, for higher waves further investigations are necessary.

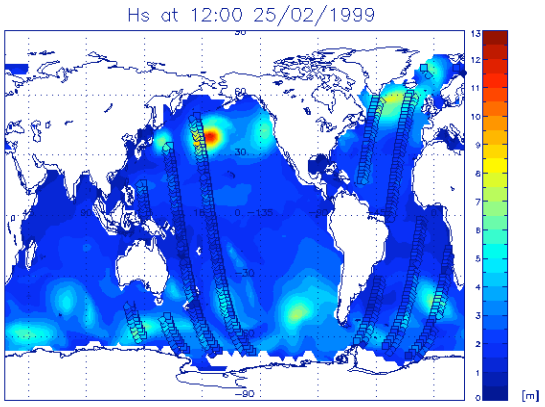

Figure 12 Map of significant wave height from ERA 40 data with superimposed measurements from the ERS altimeter (diamonds) and ERS SAR (squares) from February 25, in 1999. The measurements are taken approximately 250km apart due to nadir and side looking instruments.

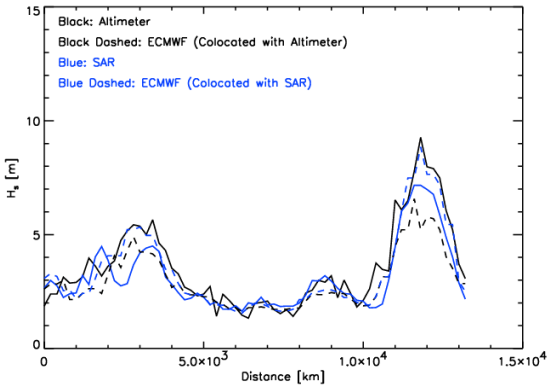

Figure 13 Comparison of significant wave height along the satellite orbit of SAR and altimeter measurements with ERA 40 results.

4.2 COMPARISON TO HOAPS RESULT

The HOAPS-II (Hamburg Ocean Atmosphere Parameters and Fluxes from Satellite Data set) contains global fields of different oceanic and atmospheric parameters (e.g. precipitation, turbulent heat fluxes, evaporation minus precipitation, wind) derived from SSM/I data over the ice free ocean. The detail about HOAPS data could be found at the website: http://www.hoaps.zmaw.de/.

Fig. 14 is a scatterplot between CWAVE SAR and HOAPS wind speed data. The large differences may be due to problems in time collocation, further investigation is needed. Fig. 15 shows an example of HOAPS wind speed superimposed CWAVE SAR.

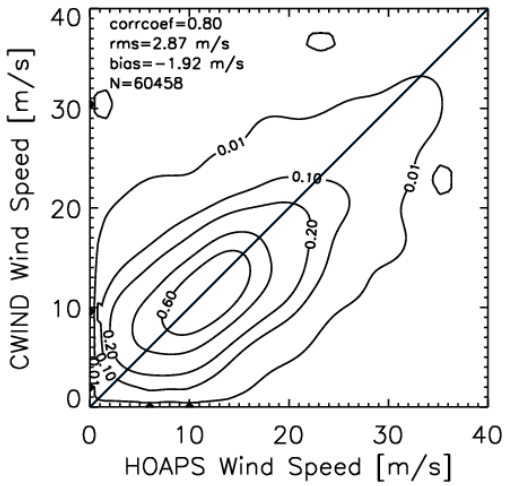

Figure 14. Scatterplot of wind speed U_{10} derived from HOAPS data against CWAVE derived SAR wind speed.

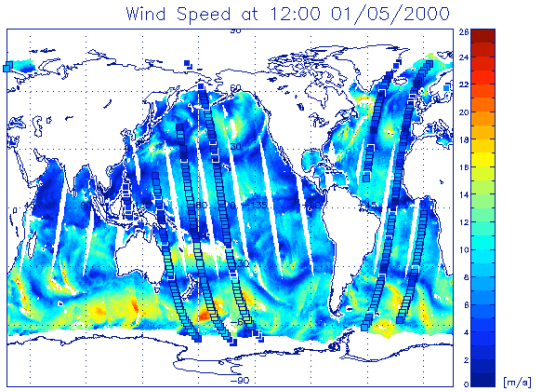

Figure 15. Map of wind speed as derived from SSM/I in the HOAPS atlas with superimposed CWAVE SAR wind speed.

5. T_{m-10} COMPARISON BETWEEN SAR RESULT AND ERA-40

The SAR yields the possibility to measure additional spectral parameters like T_{m-10}.The definition of wave mean period in this study is as following:

$$T_{m-10} = \frac{m_{-1}}{m_0} \qquad (1)$$

Where m_{-1} and m_0 are the -1th and 0th spectral moments respectively.

Fig. 16 shows the scatterplot of T_{m-10} between SAR result and ERA 40. It shows rms of 0.94 s. The correlation coefficient is 0.80. Fig. 17 shows the scatterplot of CWAVE H_s against CWAVE T_{m-10}. The typical relationship between T_{m-10} and H_s is observed.

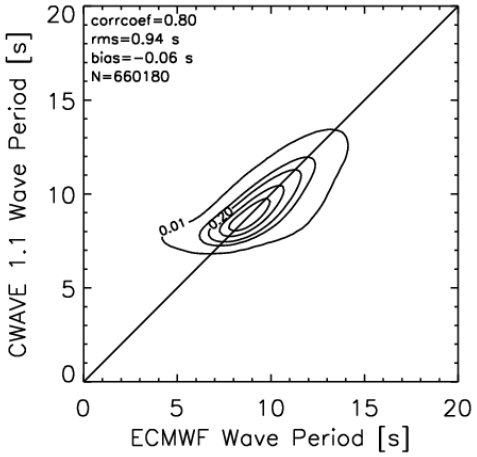

Figure 16 Scatterplot of T_m derived from ERA 40 data against CWAVE RESULT.

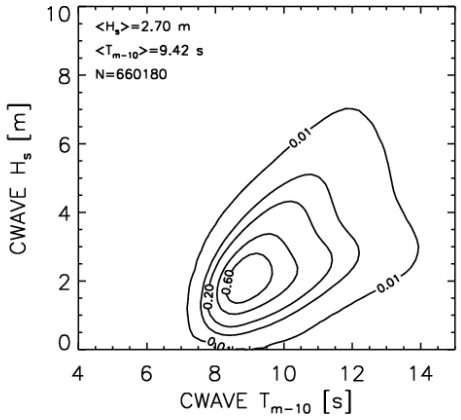

Figure 17 Scatterplot of CWAVE H_s against CWAVE T_{m-10}

6. CONCLUSIONS AND DISSCUSSION

The performance of the new CWAVE algorithm is assessed in this study. Statistical parameters like correlation, rms and bias are calculated from SAR results in comparison to other in Situ and satellite datasets. According to these statistical parameters the H_s results derived by CWAVE SAR are of the same quality as the altimeter results. The validation between SAR results and in situ data shows an rms of less than 0.5 m in H_s. Further investigations are necessary for the performance of CWAVE in high sea state. Scatterplots of H_s and T_m-10 will be derived for different part of the ocean.

Statistical analysis between SAR results and other datasets indicates that inhomogeneous imagettes affected by rain, surface films or other oceanic and atmospheric features are a critical factor, this needs further investigation.

6 REFERENCES

1. Schulz-Stellenfleth, J., König, T. & Lehner, S. (2007). An Empirical Approach for the Retrieval of Integral Ocean Wave Parameters from Synthetic Aperture Radar Data. *J. Geophys. Res*.112, 3019-3033.

2. Hasselmann, K., Raney, R. K., Plant, W. J., Alpers, W., Shuchman, R. A., Lyzenga, D. R. , Rufenach, C. L. & Tucker, M. J. (1985). Theory of Synthetic Aperture Radar Ocean Imaging: A MARSEN View. *J. Geophys. Res*. 90, 4659–4686.

3. Johnsen, H. & Desnos, Y.- L. (1999). Expected Performance of the ENVISAT ASAR Wave Mode Cross Spectra Product. Proceedings of the IGARSS 99 conference.

4. S. Lehner, J. Schulz-Stellenfleth, B. Schättler, H. Breit, and J. Horstmann. (2000), Wind and wave measurements using complex ERS-2 SAR wave mode data. IEEE Trans. Geosci. Remote Sensing, 38(9), 2246–2257.

5. König, T., Lehner, S., Schulz-Stellenfleth, J., Song, G. & Reppucci, A. (2006). Remote Sensing of Extreme Wind and Ocean Wave Fields. Eighth International Winds workshop in Beijing. April, 2006.

6. Hersbach, H., Stoffelen, A. & Haan, S. de (2007). An Improved C-band Scatterometer Ocean Geophysical Model Function: CMOD5. *J. Geophys. Res*, accepted.

7. Stoffelen, A., & Anderson, D. (1997), Scatterometer Data Interpretation: Estimation and Validation of the Transfer Function CMOD4. *J. Geophys. Res*, 102, 5767-5780.

8. Lionello, P. Guenther, H. & Janssen, P. (1992). Assimilation of Altimeter Data in a Global Third Generation Wave Model. *J. Geophys. Res*., 97, 14453-14474.

9. Horstmann, J., Schiller, H., Schulz-Stellenfleth, J. & Lehner, S. (2003). Global Wind Speed Retrieval from SAR, *IEEE Trans. Geosci. Remote Sens*. 41, 2277-2286